9th Biennial International Conference
& Exposition on Petroleum Geophysics

"HYDERABAD 2012"

P-198

CSEM and MMT in the use for sub-basalt structure outside the west coast of India

Jan Petter Morten, Stein Fanavoll, Frida Mrope, EMGS*

Summary

In the deep water areas offshore the west coast of India, thick basalt layers hamper the imaging of deep structures which are possible targets for hydrocarbon exploration. Marine controlled source electromagnetic measurements in the broadside source-receiver configuration allows mapping of base basalt and underlying structure. We study a case where the spatial resolution of magnetotelluric data is too low to map a thin basaltic layer, making CSEM an important exploration tool that can provide structural information to identify prospects and aid seismic processing. Improvements in acquisition and processing technology are shown to further extend the application envelope demonstrated in previous studies.

Introduction

Offshore the west coast of India, a major volcanic event, the Deccan Traps, dominates the subsurface and poses huge challenges to the exploration for oil and gas. This applies especially in the deep water areas, where depth to the basalt is moderate, and only few exploration targets can be identified in the post-basalt sequence. Sub-basalt plays are therefore receiving increasing interest in the exploration for oil and gas. Besides basalt acting as a direct seal for hydrocarbon accumulations, there are a variety of traps that can be hidden below a basalt layer. However, due to shape irregularities and heterogeneities with high velocity contrasts around and within the basalts, it can be challenging for seismic processing to image the base of the basaltic layer and details of what is below. Hence, methods that improve mapping of basalt and the sediments below will be of great value.

MacGregor and Sinha (2000) that the marine controlled source electromagnetic (CSEM) method can provide large-scale, low resolution structural information of basalt and underlying layers, in particular in conjunction with marine magnetotellurics (MMT), MacGregor (2003). In cases where only very low frequency MMT data is available, e.g. in deep water, broadside CSEM data can contribute the required spatial resolution from high frequency as shown by Morten et al. (2011).

India West coast

The volcanic feature known as the Deccan traps covers almost the whole part of the Indian west coast that is open for exploration. From both offshore and onshore drilling, it is known that the basalt thickness can exceed 2 km. In the shallow water areas close to the shore, the total depth to the basalt seems to increase, making the thickness of the overlying sequence sometimes exceed 4 km. In this study, we focus on the deep water areas, where the depth to the basalt ranges approximately from 1000 m to 2000 m. Most of the prospectivity is regarded to be sub-basalt, emphasising the importance of imaging the sub-basalt sequence.

Seismic data can typically image the top basalt in this area, but accurately defining basalt thickness or underlying structure can be challenging (Roberts, 2008). Of particular interest is the sedimentary section below the Deccan basalts. Basalt is typically high resistive, whereas brine saturated sediments are conductive. Due to the resistivity contrast to the basalt, electromagnetic measurements will be sensitive to the geometry and depth to sediments.

Controlled source electromagnetics

In controlled source electromagnetic (CSEM) measurements, a horizontal electric dipole source is towed close to the seafloor. Inline data is measured at receivers

EMGS ASA, Stiklestadveien 1, 7040 Trondheim, Norway
sf@emgs.com

lying along the trajectory of the towed source. Broadside data is measured at receivers having a lateral displacement from the source. We will show below that the broadside data will have enhanced sensitivity to conductive layers below basalt. State-of-the-art 3D surveys with receivers on a grid and multiple tow lines, often using a range of tow line directions, contain a rich dataset with both inline and broadside data, but require substantial vessel time to acquire. A 2D CSEM survey for early exploration stage mapping can be acquired faster, but typically deliver very limited broadside data. We study regional mapping with a 90 km long 2D CSEM line, which gives broadside data, but requires dense deployment of receivers 500 m apart. A single tow along the receiver line provides inline data, and additional, short cross-lines placed at 3km intervals along provide broadside data. The short receiver spacing assumed provides broadside data at a denser offset sampling, and reflects current capacity of modern vessels. Future developments may facilitate towing of a cross-dipole source, with which a single towing gives both inline and broadside data with larger receiver spacing.

Let us first consider the differences in sensitivity for thick resistive structures for inline and broadside CSEM data. Inline measurements are very sensitive to the presence of resistive layers, since the electrical field in that case couples to the resistor with a large vertical component. This results in a series coupling of the resistor with the conductive environment, and results in a partially guided wave event. Since the guided wave pertains also for thin resistors due to the effective series coupling, inline CSEM measurement are successfully utilized in exploration for hydrocarbons which constitute thin resistive anomalies (Constable and Srnka, 2007). However, the guiding effect reduces the sensitivity to structures below the resistor, due to the dominant guiding contribution. CSEM data from a broadside configuration, on the other hand, couple with a large horizontal electrical field and is sensitive to the resistivity resulting from a parallel coupling of layers. The broadside data, similar to MMT data, thus has limited sensitivity to thin resistors. The reduced guiding effect for broadside measurements does however imply a relatively larger sensitivity to conductive structures below.

To study the sensitivity of inline and broadside data to structure below a resistor, we consider the synthetic model shown in Figure 1. The ultra-deep water model (0.27 Ωm) has an overburden (3 Ωm) over a wedge shaped basalt layer (100 Ωm). Below the basalt there is a sedimentary layer (2 Ωm) and a non-crystalline basement (10 Ωm). The structures are invariant in the direction perpendicular to the figure. The shape of the basalt layer allows us to study the sensitivity to structures below as a function of the thickness. We expect that the sensitivity decays with increasing basalt thickness. For simplicity, we have here assumed homogeneous basalt. However as shown by MacGregor (2003), the CSEM response to a stack of thin alternating resistors is very similar to a thick homogeneous resistor with an average resistivity.

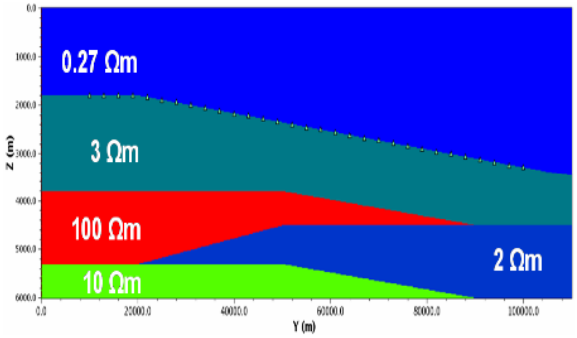

Figure 1: True model with layers from top to bottom: Seawater, overburden, basalt, sediments, and basement. Green dots show the receiver positions.

In order to analyse the sensitivity of the CSEM data, we compare data from the true model to a basalt flooded model where the sediment and the basement resistivities are replaced by 100 Ωm. This model represents the information available after a seismic survey which was only able to image the top basalt. Simulated electric field data from a current dipole source was created for the 31 receiver sites indicated in Figure 1, with receiver separation 3 km. Source positions were created each 500 m along the receiver line, with the source having two polarizations, inline and broadside. In a real acquisition, such dataset should be acquired by interchanging source and receiver positions using reciprocity. Figure 2 shows the normalized data difference between true model and basalt-flooded model, |ETrue-EFlood|/|EFlood|, common mid-point (CMP) sorted. A response at e.g. 1 in these plots means that the difference between data from the true and basalt flooded models is 100% of the data magnitude.

Consider first the plot of inline normalized data difference. The rightmost part of the model shows the strongest response because in this region the resistive layer is completely pinched out in the true model. Moving towards

the left in the figure, we see that the data difference quickly decays due to increasing resistor thickness and associated reduced penetration. Below the thickest (1.5 km) part of the resistor, the response falls to 35 % and the signal level approaches the noise level 0.1 nV/m. The data therefore has significant information about structures below the basalt also in this region, but since it is marginal, reliable imaging is questionable.

The broadside normalized data difference shows that the response is largest from the area where the resistive layer is pinched out, similar to the inline data. Moving left towards the part with thicker basalt, we see a qualitatively different behaviour than inline data. The response does not decay much with increasing resistor thickness, only a shift towards larger offset is observed. For the whole thickness interval probed by this model, the broadside data response remains large at more than 100 % with a signal magnitude above the noise level even at the farthest offset plotted.

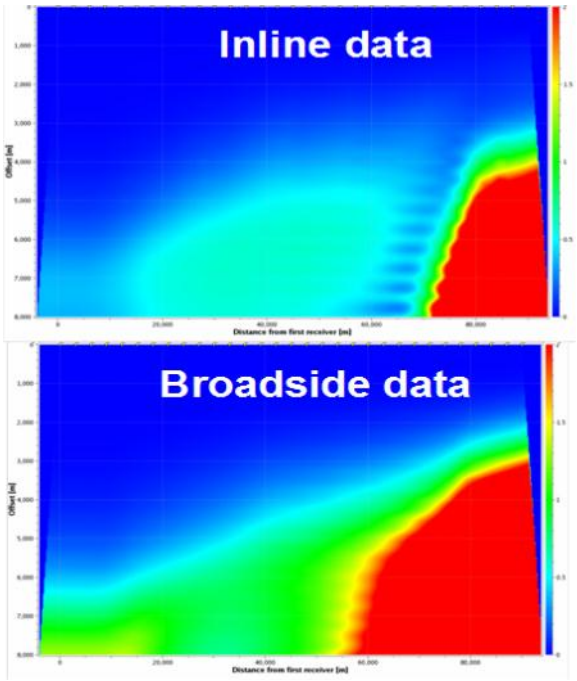

Figure 2: CMP sorted normalized data-difference at 1.5 Hz between true model and basalt flooded model. Upper plot shows inline data, lower plot broadside data.

In summary, the broadside data responses provide information about structures below the basalt three times more significant than inline data. It has a qualitatively different dependence on the basalt thickness. The response of inline data decays rapidly with resistor thickness, whereas broadside data responses remain large for the thicknesses studied here. We can therefore expect that imaging of sub-basalt structures that can utilize broadside data will yield more accurate descriptions and be more robust than imaging based on inline data alone.

CSEM inversion results

Figure 3 shows the 3D inversion result of the synthetic data based on the true model. The 3D inversion tool is described in Zach et al. (2008). To speed up the convergence, the initial model is created by 31 independent 1D inversions, one for each CMP sorted gather. Top basalt is assumed known, such that the overburden is treated as a single layer in the 1D inversion. No other regularization is employed at any stage of the inversions. We inverted the broadside and inline data at frequencies 0.6, 1.0, and 1.5 Hz. Figure 3 shows that base basalt is imaged to about 100 m accuracy when the thickness is lower than 1 km. In this region the sediments and the basement are also imaged adequately, both in terms of structure and resistivity. As the basalt thickens, imaging of the structures below becomes poorer, but the result still identifies base basalt to about 300 m accuracy. The data misfit was generally below 10 % relative to the true model data amplitude, but shows some significant residuals at far offset for the central receivers indicating that more information could still be extracted from the data.

In addition to the result shown in Figure 3, we also inverted broadside and inline data separately, as well as different frequency combinations (not shown). The inline data only inversion gives much poorer results than the broadside data only inversion, which is expected due to the difference in sensitivity discussed above. In particular, the base basalt was not imaged when its thickness exceeded 1 km.

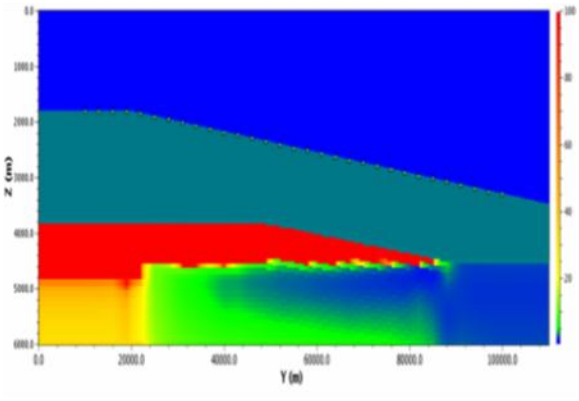

Figure 3: Final model from 3D inversion of broadside and inline electrical field data at 0.6, 1.0, and 1.5 Hz.

Marine magnetotelluric (MMT) inversion

As discussed in the introduction, MMT data has been applied to image structures below thick resistive layers. [For a recent example see Virgilio et al. (2010)]. The scenario discussed in the present paper, with ultra-deep water and a pinching out basalt layer may be challenging for MMT applications. The water depth will attenuate the higher frequency part of the MMT spectrum, which we expect to be essential for proper imaging of the thinner parts of the resistive layer. In order to study this prediction, we have performed MMT inversion using the same receiver layout as in the CSEM case and with data at 20 frequencies from 1/20 to 1/1500 Hz, a typical range observed in proprietary datasets at deep water and low latitude. The initial model was the same flooded model used for the CSEM inversion to make a fair comparison. The central section of the final model result is shown in Figure 4. The MMT inversion result lacks resolution to identify the basalt and sediment layers, but provides a good image of the basement. The data fit for this result was on the scale of the expected survey accuracy.

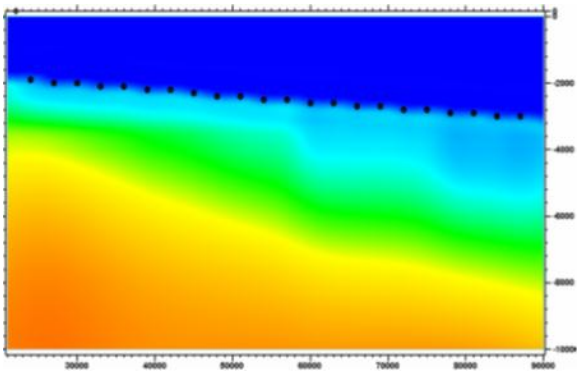

Figure 4: Final model from MMT inversion.

Conclusions

We have studied synthetic CSEM data from a model with a variable thickness basalt layer overlaying conductive structures. We demonstrated that the improved data quality and processing algorithms can enhanced the sub-basalt imaging resolution to ~100 m. The results also apply for sub-salt or sub-carbonate structures. The broadside configuration measurements show large sensitivity to the conductive structures even when the basalt layer is as thick as 1.5 km, and inversion of the data demonstrates how CSEM can be utilized to map base basalt and even image the sediments and basement below. At the same time we show that MMT data in a deep water environment will inadequate resolution to reliably identify the structures. Thus the broadside CSEM data provides exclusive information to assess possible reservoir prospectivity in environments where basalt layers may cover conductive reservoir rock. Information about base basalt will also provide better velocity models that improve seismic processing and imaging.

Offshore west coast of India, the Deccan Traps is a major obstacle to properly image deep structures. The application of CSEM is, however, useful in deep water areas where the depth to the base of Deccan Trap is well within the sensitivity for the technology. In shallow water the depth to base of Trap could easily exceed 6 km, and possibly be beyond sensitivity for CSEM, and less attractive as drilling target. Future development in source and receiver instrumentation could however change this.

References

Constable, S. and Srnka, L.J. [2007] An introduction to marine controlled-source electromagnetic methods for hydrocarbon exploration. Geophysics, 72, WA3-WA12.

Fliedner, M.M. and White, R.S. [2001] Seismic structure of basalt flows from surface seismic data, borehole measurements and synthetic seismogram modelling. Geophysics 66, 1925 (2001).

MacGregor, L., and Sinha, M. [2000] Use of marine controlled-source electromagnetic sounding for sub-basalt exploration. Geophysical prospecting 48, 1091 (2000).

MacGregor, L. [2003] Joint analysis of marine active and passive source EM data for sub-salt or sub-basalt imaging. 65th EAGE Conference & Exhibition, Expanded abstract F18 (2003).

Morten, J.P., Fanavoll, S., Mrope, F.M., and Nguyen, A.K. [2011] Sub-basalt Imaging Using Broadside CSEM. 73rd EAGE Conference & Exhibition, Expanded abstract C029 (2011).

Roberts, G. [2008] Deepwater West Coast India. GeoExPro November 2008.

Virgilio, M., De Stefano, M., Re, S., Golfè Andreasi, F., and Snyder, F.F.C. [2010] Simultaneous Joint Inversion of Seismic, Gravity, and EM Data for Subsalt Depth Imaging in Gulf of Mexico. 72nd EAGE Conference & Exhibition, Expanded abstract K045 (2010).

Zach, J. J., Bjørke, A. K., Støren, T., and Maaø, F. [2008] 3D inversion of marine CSEM data using a fast finite-difference time-domain forward code and approximate hessian-based optimization. SEG Expanded Abstracts 27, 614(2008).